EPJ Web of Conferences **263**, 01013 (2022) https://doi.org/10.1051/epjconf/202226301013
8th Complexity-Disorder Days 2021

Symmetry Breakings in the interactions of Molecular Hydrogen with Solids

Ernest Ilisca[1,2*], *Loïc* Houssais[3], and *Filippo* Ghiglieno[4]

[1] Université de Paris, France
[2] SHYT, Storage of Hyperfine Hydrogen for Transport, France
[3] Acadomia, Rennes, France
[4] Laboratório de Óptica, Laser e Fotônica, Federal University of São Carlos, Brazil

Abstract. The following conference report considers hydrogen gases with odd and even rotational quantum number as two separate gases, the ortho and para varieties which do not interconvert in absence of a catalyst. The physical catalysis of hydrogen is interpreted in terms of symmetry breakings introduced by the solid to pass round the peculiar selection rules of the molecular hydrogen assigned by the Pauli Principle. The catalytic effect presents the striking effect of reducing drastically the interconversion time, longer than the age of the universe for isolated molecules, to a few seconds or minutes when an hydrogen sample (gaseous or liquid) is brought into contact with an efficient catalyst. In the present report, the variety of new optical and electronic devices, measurements and interpretations that have been reported since the turning of the new century are reviewed. New experiments on non-magnetic catalysts measuring hydrogen conversion on the time scales of one-ten minutes turned upside down the previous theory, established in 1933, of the absolute necessity of a magnetic catalyst to break the Pauli Principle. The o-p catalyzed reaction is discussed for hydrogen molecules adsorbed on electric surfaces, or in confining porous structures or inside nanocages. New concepts and new electromagnetic conversion channels that interpret these experimental renewals are described in terms of how the hydrogen nuclei feel the solid-molecule electron cloud complex. The described channels differentiate one another owing to the catalyst and owing to the electronic path followed in the configuration space by the o-p reaction.

1 Introduction to the Physical Catalysis of molecular Hydrogen

1.1 Hydrogen molecules have the peculiar and seldom property of a quantum structure macroscopically observable at room temperature. It is possible to distinguish those molecules which have their proton spins parallel or antiparallel and these modifications have been diversely denoted spin isomers, or spin manifolds or ortho (o) and para (p) varieties in the past [1-4]. A hydrogen gas is thus composed of a mixture of these two varieties of definite ratio when it is equilibrated with a thermostat at a fixed temperature. However non equilibrium mixtures are stable for very long periods, during which each variety equilibrates separately with the thermostat but not each other. From almost a century, hydrogen was and still is practically converted practically to thermodynamic proportions by passing through a magnetic catalyst, since only local magnetic gradients were known able to break the spin and rotational nuclear selection rules [5-6]. Such catalysis was denoted as “physical” in order to distinguish it from the “chemical” one where the molecular electronic bond being broken or at least admixed within the catalyst electronic charge [1]. The physical conversion of one variety into the other is currently observed while the molecular integrity remains unaltered. The magnetic mechanism that uncouples the two proton spins was believed to be the unique process able to convert and relax a hydrogen mixture toward equilibrium. However, since the new century non-magnetic catalysts were shown able to convert molecular hydrogen samples and it appeared necessary to reformulate and enlarge the theoretical approach of the conversion mechanism. The catalytic process can be characterized by a simple fundamental and double o-p selection rule: $\Delta J = \Delta I = 1$, where J and I are respectively the rotational and nuclear spin angular momentum quantum number of the hydrogen molecule. In the magnetic mechanism both selection rules are satisfied simultaneously in a single reaction. However, it has been demonstrated in 1986 that the conversion process might be achieved in a few successive steps that complement each other [7]. By interpreting new "in situ

* Corresponding author: ernest.ilisca@gmail.com

and real time" experiments new conversion channels were discovered [7-9].

The purpose of that paper is to describe in simple terms the various channels, explicit their discovery and classify these in function of the number of catalytic steps necessary to fulfill the double o-p selection rule: $\Delta J = \Delta I = 1$. In this respect the catalytic process appears as a "Symmetry Breaking" operation of the selection rule imposed by the "Pauli Principle".

In the following introduction the fundamental symmetries which are at the origin of the ortho and para varieties are clarified and the historical background of the conversion phenomena recalled. The next chapter 2 describes the various conversion channels whereas the chapter 3 characterizes them in terms of the successive symmetry breakings introduced by the catalyst. The chapter 4 summarizes the various and recent experimental investigations and stresses the renewal of methodology. Finally, a few concluding comments are devoted to present and future prospects in various fields.

1.1 Molecular Hydrogen symmetries

In order to simplify the description of the quantum structure of the hydrogen molecule the orbital basis will be limited to a full bonding state and an empty antibonding one, without any loss of generality. The symmetry of the electron system under the inversion and permutation group distinguishes the even state g (gerade) from the odd state u (ungerade), whereas the Plane Reflection symmetry attributes a sign to each molecular state (+ / -). The hydrogen ground state $^1\Sigma_g^+ = |g\bar{g}|$ considers that the bonding $g = \sigma_g(1s)$ molecular orbital is filled by the two electrons in a spin singlet configuration because the Pauli Principle, applied to the fermions, associates the spin anti-symmetry to the orbital symmetry by electron exchange (electrons pair in closed-shell restricted orbitals). The first excited electronic state $^3\Sigma_u^+ = |gu|$ associates the symmetry of spin-triplet to the orbital anti-symmetry of the anti-bonding state $u = \sigma_u^*(1s)$. The first two levels energies of the Electronic Excited Spectrum are represented in the Figure 1 as a function of the internuclear distance.

It is apparent on the Figure 1, and well known, that the $^3\Sigma_u^+$ excited state is unstable and leads to the molecule dissociation. However, when the molecule interacts strongly with a solid it mixes with the solid electrons and partially fills. In the following such a mixing will not be considered as real but only virtual; that is as a possible transient path in the electronic reaction. Most of the bonding density is spherical while the antibonding one is directed along the inter-nuclear axis ab. It remains empty for a free molecule. Its progressive filling weakens the hydrogen bond when chemically adsorbed on a surface [10]. It allows important reaction paths in chemisorption and plays a key role in the conversion of hydrogen interacting with a solid. Such a molecular antibonding state has a strong electron-nucleus hyperfine contact because of its 1s atomic content of finite amplitude at the protons. Note that the molecular and solid electron clouds slightly overlap, and consequently, the fundamental ground state of the molecule-solid electron complex must be described at zero order by the anti-symmetric product of the separate ground states: a total singlet, represented by a Slater determinant.

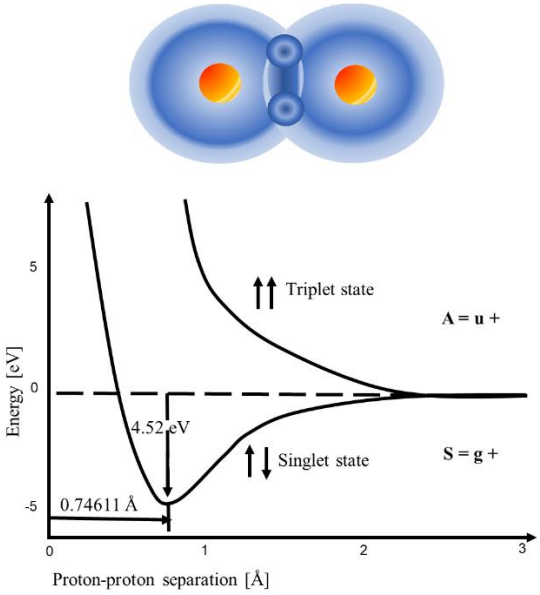

Fig. 1. Molecular hydrogen electron symmetries. Above: the fundamental electron cloud; under: the energies of the first two molecular electron states in function of the proton-proton separation

That property of eigenstates totally antisymmetric with respect to electron permutation is even stronger for the neutral and ionic antibonding excited states.

1.2 Nuclear symmetries: ortho and para isomer varieties

Inverting the position of the nuclei changes also the electron positions and the permutation of the electrons changes the sign of the wave function. Consequently, nuclear spin and rotational parities are associated owing to the parity of the electron state. The existence of the nuclear spin isomers: ortho (o) and para (p) varieties of molecular hydrogen illustrates the Pauli Principle applied to the protons: the total wave functions of molecular hydrogen must belong to the alternate representation of the permutation group of the nuclei [2-4]. In the fundamental X $^1\Sigma_g^+$ state (where the inversion of electrons is gerade and the reflexion through a vertical plane positive), the spin and rotational states have opposite parities. The required anti-symmetry of the two-proton states associates the odd rotational states to nuclear triplet spins, denoted **ortho**, and even rotational states to singlet spins denoted **para**. The ortho states are thus defined by (**o**; J odd and I=1) and the para ones by (**p**; J even and I=0). (J and I denote the rotational and spin nuclear momenta).

Contradistinctly, for the odd (and +) electronic terms the nuclear coupling is opposite: the antibonding state $u = \sigma_u^*(1s)$, orthogonal to g and odd under inversion, associates differently rotational and nuclear spin states of identical parity: J is even (resp. odd) for triplet (resp. singlet) nuclear spins. For the first two levels of Σ_u^+

(J=0, I=1) and (J=1, I=0). In that way, the electron and nuclear symmetries (space and spin) of the ortho and para states are intricately linked. In particular for the ortho variety the hyperfine interactions incorporate some electron magnetism inside the ground state.
The low energy part of the rotational spectrum is represented on the Figure 2 and a pictorial representation of the first two ortho and para states on the Figure 3.

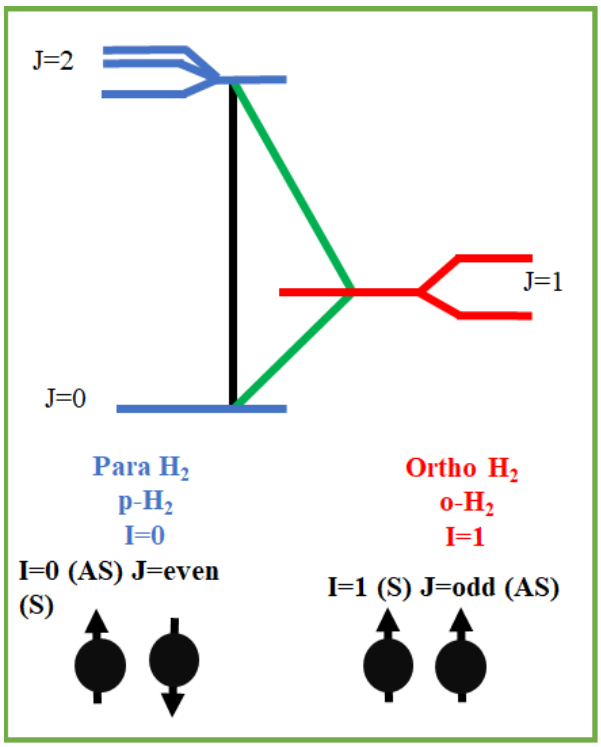

Fig. 2. Nuclear rotation and spin manifold in the $^1\Sigma_g$ fundamental ground state where the Ortho manifold associates the rotational J Odd states to the even spin triplets: I=1 whereas the **Para J Even** ones are associated to the odd spin singlets **I = 0** (Only the first three levels are represented).

The rotational space being divided in two subspaces corresponding to the two ortho and para manifolds {o, p}, they manifest their properties as two different isomers (or varieties) and in some respects as two different gases of different specific heats and different nuclear magnetism.

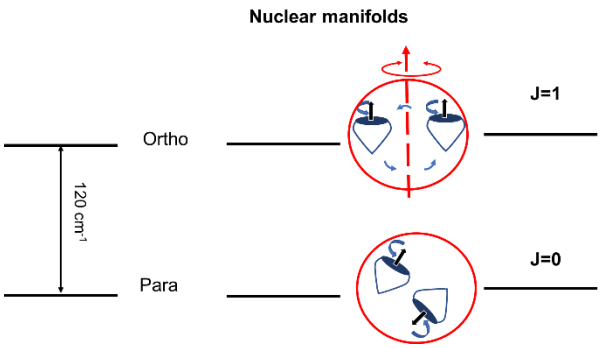

Fig. 3. Nuclear ortho and para rotation and spin manifolds

Although the total nuclear spin manifolds, I=0 or 1, result from the angular addition of the two protons half integer spins: $|(½,½)Im_i>$, their energy differences are related to the overall molecular rotation and fall in the far infra-red region. In particular the first two ortho and para states (J=I=1) and (J=I=0) are about 118 cm^{-1} =172 K = 14,7 meV apart. At room temperature only these two levels are mainly occupied.

1.3 Conversion historical summary

The problem of the hydrogen molecule was a hot topic in early 1927 at Copenhagen between Bohr, Hund and Hori. But it was a young scholar, Dennison, that succeeded in calculating the right specific heat by considering the gas with odd J and the gas with even J as two separate gases which do not interconvert. He pointed out for the first time that the mixing ratio of 1/3 is the mixing ratio of the two « J-even » and « J-odd » gases at room temperature and concluded that this means that the proton is a fermion of spin ½. Giauque confirmed in 1928 Dennison idea of a frozen equilibrium (because the transition between solid and "dashed" levels takes a long time) by keeping a sample of hydrogen for 6 months. The observed vapor pressure change was very slow, and one year later, Bonhoeffer and Harteck successfully catalyzed the attainment of equilibrium, and isolated one of the hydrogen « modification ». At about the same time, Eucken and Hiller observed the specific heat changes for samples cooled down to low temperature. The following Table 1 summarizes the parallel evolution of the quantum theory and conversion discovery as well as their industrial applications.

Table 1. Historical background.

1925	Electron Spin	G. E. Uhlenbeck and S. A. Goudsmit
1925	Symmetry Principle	Wolfgang Pauli
1926	Fermi-Dirac Statistics	Dirac - Heisenberg – Pauli - Fermi
1927	Nuclear Spin	David M. Dennison
1929	ortho and para H_2	Bonhoeffer - Harteck, Eucken - Hiller
1933	Magnetic Catalysis	E.P. Wigner
1950	Ferric Iron Oxide Catalysts	NBS
1960	Program Apollo	NASA
-	Industrial Liquefaction	Lindé – Air Liquide

For a long time, conversion measures were performed by calorimetric or nuclear magnetic resonance methods [1,11-13]. More accurate methods appeared in 1992 when Raman and infrared spectroscopies could observe

the hydrogen conversion by exciting the molecular rovibronic degrees of freedom [14]. Hydrogen conversion is neither spontaneous (ortho or para lifetimes of isolated molecules are comparable to the age of the universe) nor induced by some direct radiation (the hydrogen molecule has no electric dipôle moment). It necessitates a catalyst to break the 2 selection rules : the nuclear spin and rotational angular momenta parity changes. In order to appreciate the historical importance of the conversion mechanisms, let us sketch a short survey.

1930-50: Shortly after the discovery of the hydrogen spin isomers, Wigner's theory [5] has allowed the interpretation of a large variety of experimental measures. It is based on the inhomogeneous magnetic field produced by a magnetic moment, able to uncouple the nuclear spins of a nearby hydrogen molecule.
1950-70: Hydrogen conversion became an industrial challenge because almost all liquefied and stored hydrogen has to be converted (around 1010 kg/year, a major part of which for aerospace rocket and engines) [6,15]. Hydrogen is practically converted to thermodynamic proportions, up to now, by passing through magnetic catalysts. Transition metal oxides, in the form of powders or beds…, were studied extensively by the NBS labs who elaborated the best catalysts for industrial purposes [16,17].
1970-80: The efficiency of weak ferro- and antiferromagnetic catalysts, as well as the discontinuities of the conversion rates at the transition temperature were interpreted on the basis of a resonant effect, where the catalyst spin-waves evacuate the molecular angular momenta and energy [18-23]. Recent experiments on insulating chromia catalysts support that interpretation while o-p hydrogen conversion is becoming a valuable tool to observe surface magnetic and electronic phase transitions [24].
1980-90: The exchange-contact XY channel discovered in 1986 has shown that electrostatic Coulomb interactions between the adsorbed molecular electrons and those of a surface paramagnetic ion compete favorably with the dipolar conversion [7]. These channels take advantage of the symmetry-breaking properties of the electron-nuclear Fermi contact internal to the molecule. Surprisingly quite fast conversion was observed in 1982 on non-magnetic noble metals, separately in IBM [25] and Chalmers [26], and later on graphite [27]. Although the experiments by EELS could not measure precise conversion rates, these experiments have established the primary observation of conversion on non-magnetic catalysts without chemisorption.

2 Conversion channels and electro-nuclear paths

That chapter is devoted to the theoretical concepts that have emerged recently in the analysis of the new Catalytic Paths and supports the conversion mechanism as an electromagnetic process. We review the conversion channels that have been discovered and studied successively in the past. The magnetic one is of historical importance. But it remains active even now since all industrial applications use magnetic converters such as in hydrogen liquefaction and large-scale storage factories. Second the metallic channels discovered on the noble metals in 1982 for silver and copper catalysts are now studied on gold samples. Third the new channels experimented on semiconductor and insulator catalysts opened a new branch of the conversion history.

2.1 Magnetic conversion

The Dipolar Process D. The considered magnetic dipolar interaction between the catalyst electrons and the 2 nuclear spins of an adsorbed hydrogen molecule is composed of the dipolar couplings between the 2 nuclear spin momenta of the hydrogen nuclei $\boldsymbol{i}^1(p)$ (p=a and b) and the spins of the catalyst electrons α: $\mathbf{s}^1(\alpha)$. The dipolar spin-hamiltonian can be written in tensor form as a sum of scalar products between a nuclear tensor $\mathbf{N^2}$ and an electronic one $\mathbf{E^2} = \sum_\alpha \mathbf{E}^2(\alpha)$. The nuclear spin difference: $\mathbf{i^1} = \mathbf{i}^1(\boldsymbol{a}) - \mathbf{i}^1(\boldsymbol{b})$, and the inter-nuclear orientation $\mathbf{ab}$ composes the nuclear tensor: $\mathbf{N^2} = [\mathbf{i^1} \times \mathbf{ab^1}]^2$, which pertains on the molecule nuclear spins and rotational degrees of freedom. Because it is odd in the permutation of the protons both in space and spin, it induces the o→p transition Δ J = Δ I = 1 in one step. The electron tensor operates on the electrons spin and orbital degrees of freedom. The electron states of the catalyst ionic centers are best referred to the solid laboratory frame. The molecular center position with respect to the fixed crystalline sites, and functions of it, are considered as thermal bath random classical variables. They describe the molecular adsorption and motion, in particular vibrations perpendicular to the surface and gas-adsorbate exchanges as well as the catalyst phonons. The Figure 4 represents the magnetic field lines of a catalyst dipole that exerts a torque on a nearby hydrogen molecule. Such a magnetic field must be sufficiently inhomogeneous to uncouple the two hydrogen nuclear spins. Therefore, the molecule and the catalyst center must be very close, less say than 4 Å. In particular an homogeneous magnetic field does not affect directly the conversion. The first microscopic analysis of the conversion process on a catalyst surface has been given by Ilisca in 1970-2 [18-21], where the details of the dipolar model can be found. In such a model, and in following publications of 1970-90 period [28-31], the magnetic dipole is assumed to be localized at catalyst centers. Further extensions that consider the spatial distribution and extension of the catalyst electrons appeared later [32-38].
The question of the energy transfers between the hydrogen molecules and the catalyst were approached soon in 1970 [4,5,18] but are still open and subject of controversy. The important o-p rotational energy might be evacuated by molecular kinetic energies or by the catalyst excitations. Different models have been investigated which involve phonons, magnons, electron-hole pairs…, depending on the experimental configuration.

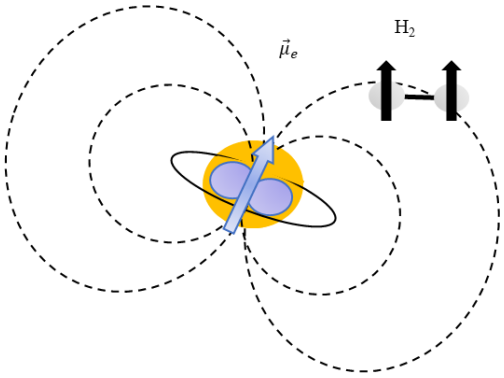

Fig. 4. Hydrogen conversion on para-magnetic surfaces: magnetic impurity dipole field.

Electron-Nucleus Hyperfine Contacts Y. The hyperfine contact between the electrons α and the hydrogen protons p allows also a transfer of angular momentum between the nuclei and the electrons [2-4,7]. Its antisymmetric part with respect to inversion introduces the nuclear spin difference: $\mathbf{i}^1$ which is the key nuclear spin operator that induces the molecular o-p conversion. It has been demonstrated that the contact interaction is particularly strong when the molecule and catalyst electron clouds overlap as occurring when the catalyst electrons extend outside the surface plane [32-35]. The contact interaction manifests also its influence by mixing the ground singlet $^1\Sigma_g$ and the excited triplet $^3\Sigma_u^+$, as illustrated by the simultaneous "flip-flop" transition of the electron and nuclear spins represented on the Figure 5.

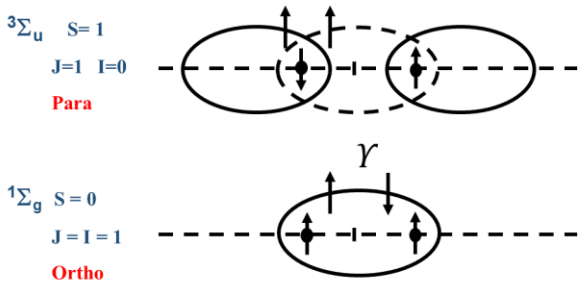

Fig. 5. The simultaneous "flip-flop" transition of the nuclear and electron spins that mixes the ground singlet and the excited triplet.

The contact Hamiltonian $\mathbf{Y} = \mathrm{Y}\,\mathbf{i}\,.\,\boldsymbol{\sigma}$ exhibits in particular a product between electron and nuclear spin difference operators that induces a simultaneous singlet-triplet transition in the electron and nuclear spin manifolds that connects the fundamental singlet to excited triplets. The hyperfine contact connects mainly the "s" electrons with the nuclei. Here arises a new concept in conversion theory. The dipolar mechanism is based on different values of the magnetic field at the 2 protons. In the contact mechanism they have the same intensity but opposite directions. Inside one electronic state the electron density is measured by the squared absolute value of the wave function, linking even and odd molecular states, and products of these have opposite signs at the 2 protons.

2.2 Metallic physical conversion

Surprisingly quite fast conversion was observed in 1982 on non-magnetic noble metals, separately in IBM [25]and Chalmers [26], and later on graphite [27]. EELS observations (Electron Energy Low Spectroscopy) of fast conversion rates of physisorbed hydrogen allowed the discovery of a new kind of metallic catalysis leaving the molecule free of any bond. Although the experiments by EELS could not measure precise conversion rates, these experiments have established the primary observation of conversion on (i) non-magnetic catalysts (ii) metals without chemisorption (iii) single crystals covered by freely rotating hydrogen molecules. The EELS experiments of hydrogen adsorbed at low temperatures on noble metals were interpreted in 1991, by the Coulomb interactions at the surface [39]. The emission of electron-hole triplet-pairs were shown to be able to carry away the ortho-para (o-p) rotational energy and their nuclear angular momenta [39-44]. It was predicted that (i) conversion should occur in about 1-10 minutes, and not hours or days as previously estimated [42-44], (ii) an applied laser could enhance the rates [39]. Both theoretical predictions were confirmed in 2003. Precise experiments of hydrogen physisorbed on Ag at low temperature, based on photo-desorption and molecular ionization confirmed the theoretical model [45-47].

2.3 Conversion in insulating media

The experimental proof of fast conversion on non-magnetic metals had been attributed to the opportunity offered by the conduction band to emit low energy magnetic excitations. Therefore, measurements of quite fast o-p conversion (of the order of one or a few minutes) of hydrogen physisorbed on a variety of dielectric and diamagnetic insulators, raised the need to reconsider the fundamentals of the theoretical catalytic framework. Briefly the insulators gap was considered as insurmountable. That new chapter of the conversion history occurred at the turning of the century when the rotational scattering of H_2 molecules interacting with a solid became measurable [14]. More precisely "in situ" infra-red (IR) spectroscopy [48-52] and photo-ionization (REMPI) [45, 53-56] associated to desorption processes induced either by thermal or laser pulses offered new means to follow the catalytic processes. These new and beautiful experiments will be discussed more extensively in the chapter 4.
For the present section, we concentrate on the Electro-Nuclear Paths that have allowed the discovery of new Conversion Channels. The hydrogen molecule is represented on the Figure 6 in its erratic motion when colliding a solid potential wall. The catalyst valence ξ and conduction η wave-function tails are exponential outside the solid whereas the molecule bonding electron g is spherically distributed around its center of mass. The antibonding orbital u is assumed to be axially spread along a symmetry axis directed toward the surface. It appears clearly that the antibonding excited states of the molecule and the solid have important overlap. They provide efficient reaction paths to convert hydrogen

molecules interacting with non-magnetic solids in time scales larger than one or a few minutes. The conceptual origin of that interpretation relies on the magnetic excitations of non-magnetic catalysts (and of the hydrogen molecule, as well). These electron excitations of triplet spins use the molecule and solid antibonding states of appreciable surface extension.

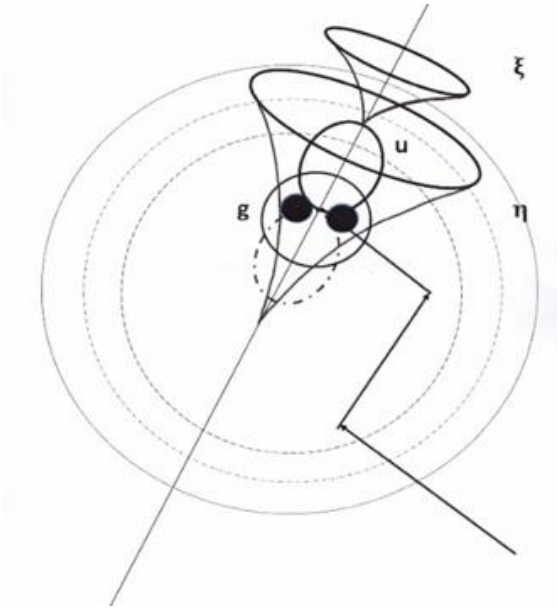

Figure 6: The Scattering. One hydrogen molecule whose center **m** follows a fast and erratic random walk inside a solid potential well is represented at a moment when the molecule scatters the solid. The molecule is represented by the two protons and its internuclear axis. The 2 molecular electrons are distributed in the bonding and almost spherical **g**(1s) state. Dotted circles figure the solid well equipotential. The empty molecular antibonding **u**(1s) state, figured by an ellipse, approaches higher potentials (repulsive hard wall). A pair of conduction **η** and valence **ξ** state exponential tails of axial symmetry are directed towards the molecule. The excited state **η** has a much larger extension and overlaps appreciably with the molecular antibonding state.

In the case of physisorption herewith considered, the antibonding u whereas empty is admixed within the solid conduction band, because of reciprocal spatial extension. First and important sizable and measurable effect, the molecule acquires a small electron dipole and becomes IR active. Moreover, the fluctuation energies are important during the short times when the molecule scatters the hard repulsion branch of the catalyst. The inter-nuclear distance is enlarged and fluctuates, and some electronic charge might then be transferred or exchanged between the solid and the molecule [57]. In other words, the fundamental hydrogen ground state does not remain completely bonding in presence of a solid and the surface electron complex contains also ionic species.

The adsorbed molecule interacts electrostatically with the whole solid, mixing their Bonding and Anti-Bonding Electronic States. Hydrogen adsorption on surfaces, or dilution within the solid, breaks the molecular inversion symmetry and induce electron transfers between the solid and the molecule, back and forth. The admixture of the antibonding molecular state with the conduction band, allows a partial delocalization of a molecular electron in the solid and inversely a partial localization of a conduction electron on the molecular edge. That « bridge » facilitates the hyperfine contact of the electrons with the hydrogen protons. The repulsion performs the molecular rotation transition by excitation of higher orbital momenta states, while the consequent electron delocalization enhances their contact with the nuclear spins.

The "Molecule-Solid" electron bondings and anti-bondings in the Electron Complex are represented on the Figure 7. Their relative admixtures depend on the position of the solid gap with respect to the molecular bonding-antibonding one: ε_{gu}. Note that the solid eigenstates are naturally expressed in the laboratory frame, whereas the molecular ones g and u, are referred to a frame attached to the molecule. When an electron is promoted from the VB to CB it leaves a hole behind, while interacting with all remaining electrons. Such excitons might be of singlet or triplet spins (3-fold spin degeneracy, m_s= 0,±1) owing to the relative orientation of the unpaired electron spins [42]. They differ mostly by an exchange energy.

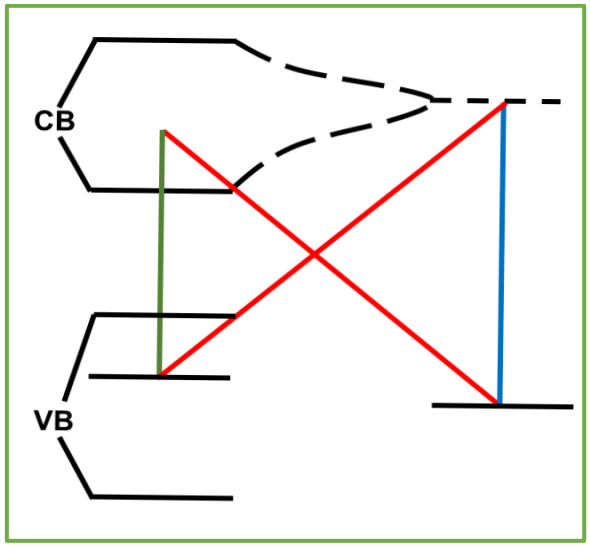

Fig. 7. Bonding-Antibonding Mixings.At zero order, the solid electron basis $\{\alpha\}$ is composed of a full valence band ($\xi \in$ VB) and an empty conduction one ($\eta \in$ CB). The molecular one has a full bonding state: g and an empty antibonding one: u (g= σ_g(1s) and u= σ_u*(1s)). By solid-molecule perturbations, four bonding-antibonding mixings are operating and involve excitation energies: (i) interbands: $\varepsilon_{\xi\eta}$, purely molecular: ε_{gu}, or charge transfer towards the solid: $\varepsilon_{g\eta}$, or towards the molecule $\varepsilon_{\xi u}$. (The molecular bonding energy: ε_g lies deeper than represented, $\varepsilon_g \approx$ - 15,8 eV). The dashed curve represents the "dressing" of the molecular antibonding u state by the conduction electrons.

In addition to the two essential ingredients of the electronuclear interactions that are the root of the conversion process, the Coulomb repulsion between the solid and molecule electrons and the hyperfine contact with the hydrogen protons, a third interaction must be added: the spin-orbit ones. An important part of the numerous electron spin polarization and spin-orbit couplings can induce mixtures between the bonding and antibonding states, either in the molecular or solid space.

These might be represented by a first rank tensor: $\mathbf{\Lambda} = \sum_\alpha \eta_\alpha(\mathbf{E})\, \boldsymbol{\sigma}^{\mathbf{1}}(\alpha)\,.\, \mathbf{l}^{\mathbf{1}}(\alpha)$ that mixes the spin and orbital catalyst electron degrees of freedom assuming that an important part of the two-electron couplings have been included inside through a mean field average. The non-diagonal operator $\boldsymbol{\sigma}$ couples singlet and triplet states while the orbital momentum $\mathbf{l}$ couples the valence and conduction bands as well as the molecular g and u states. The strength of that interaction might be enhanced by the surface electric field E, as first noticed by Fukutani [56]. Such spin-orbit interaction might be predominantly static as encountered in spin relaxation processes or dynamic as occurring in triplet-triplet annihilations of delayed fluorescence. In the following Figure 8, the hydrogen molecules are represented (in red) confined within nanocages (inside buckyballs, fluorenes or interstitial semiconductor cages). Every collision of a molecule against the hard repulsion wall of the cage induces either an excitation or a relaxation of the molecule which thereafter might propagate and disintegrate a little further ahead.

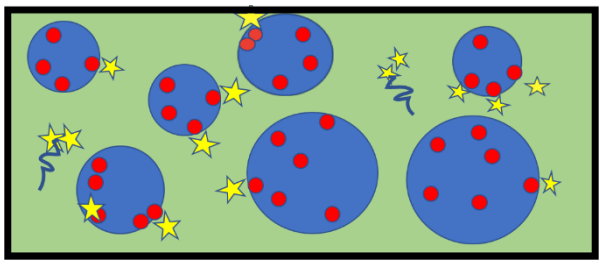

Fig. 8. Electromagnetic Conversion channels in semiconductors and insulators. The hydrogen molecules in red are confined inside the blue nanocages, while the excitonic propagations (yellow stars) diffuse through the catalyst before being disintegrated by mutual collisions.

3 Catalytic steps and symmetry breakings

The old Wigner theory, based on a catalyst magnetic ground state exerting an inhomogeneous magnetic field and torque on the molecule to uncouple the nuclear spin precessions, cannot provide a useful framework to interpret the numerous observations of hydrogen conversion on non-magnetic solids. The difficulties encountered in elaborating a theory large enough to model non-magnetic hydrogen catalysis are conceptual and related to the large variety of observations. Main questions to answer are as follows:

- Is it possible to build a theory that interprets the conversion measures according to the solid properties (insulating or metallic, surface electric gradients…), the scattering geometry and the thermodynamic variables (T, P, n...)?
- How to display and correlate a variety of patterns of different time scales: electronic (from femtoseconds to nanoseconds) to nuclear ones (from about one minute to hundreds of hours)?
- How to describe and relate in a simple form the very local (over less than one Angström) and energetically weak nuclear hydrogen conversion (about 15 meV) to the solid electron fluctuations, which are extended, collective and energetic (over the eV)?

In the Figure 9, we have represented schematically the different interacting systems of the solid-molecule complex: T is the thermal bath of the adsorbed molecules and solid phonons, subjected to an operator that might change the temperature and the conditions of the scatterings, S represents the orbital and spin electronic angular momenta of the complex. J and I are the nuclear rotational and spin hydrogen system.

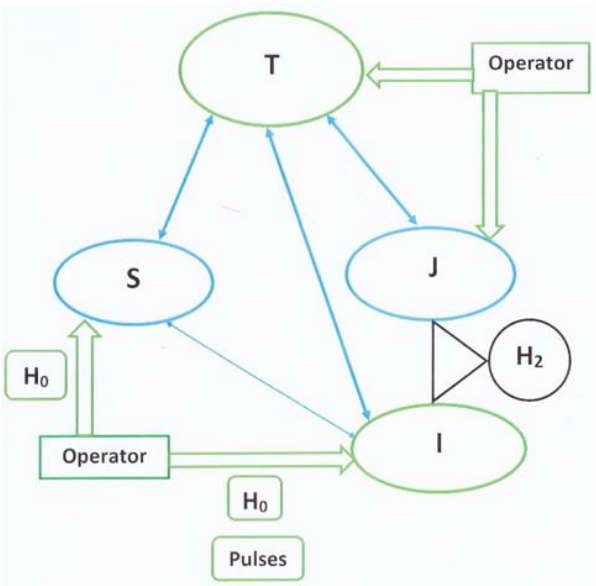

Figure 9. T is the thermal bath of the adsorbed molecules and solid phonons, S represents the orbital and spin electronic angular momenta. J and I are the nuclear rotational and spin hydrogen system. The operator controls the temperature, the conditions of the scatterings and might apply magnetic fields and radiative pulses.

3.1 Conversion channels and catalytic paths

The associated molecular conversion by a catalyst must satisfy the fundamental o-p selection rule: $\Delta J = \Delta I = 1$, but such a conversion might be achieved in a single reaction interaction that complement each other successively.

3.1.1 One – Step Channels

The magnetic couplings, either dipolar or contact, between the catalyst electrons (mainly their spins) and the hydrogen nuclear magnetic momenta are able to convert the molecule in a single and real step. The two nuclear (spin and rotation) selection rules can be simultaneously satisfied. In paramagnetic conversion, the stronger the electron spin S is, the faster is the nuclear conversion through the selection rule of the 3 angular momenta (S_i=S,1, S_f=S), and in that $\Delta S = 0$ case the rate is proportional to S(S+1). It has been verified by many experiments on surfaces [1-5,58-60], in solutions [12,13,61-67], and demonstrated theoretically [29-34]. In any case for paramagnetic catalysts the catalytic magnetic path satisfies the 2 nuclear selection rules simultaneously $\Delta J = \Delta I = 1$: **(J = I = 1) → (J = I = 0).**

3.1.2 Two– Step Channels

Each channel is a reaction path "℘" that corresponds to a tunneling through a particular barrier. The Coulomb-Contact **CY,** considers the electrons and nuclei as inter-dependent systems. A spin-triplet exciton is emitted in the solid, by a transfer of a valence electron to the conduction band and travels around until annihilation. That emission might be achieved by electron exchange **C = X**, or electron transfer towards the molecule **C = U**, or towards the solid **C = V**. Each transfer is complemented by a different contact **Y** between the electrons and the nuclei. Since the nuclear and electron angular momenta (and energy) transfers are simultaneous, the conversion occurs at the high frequencies of several eV.
The Two–Step **XY** Channels were investigated first to interpret the hydrogen conversion during their adsorption on alumina catalyst with chromia impurities dispersed on their surfaces. These catalysts are used commercially on a wide scale and the dipolar magnetic mechanism was found insufficient to interpret the observed catalytic rates. It was then adapted to the metallic silver and copper cases by introducing charge transfer processes mainly from the metal towards the molecule: the so-called UY process. The Figure 10 represents the **XY** Conversion Process (Electron Exchange **X** and Hyperfine Contact **Y**) of a hydrogen molecule interacting with a diamagnetic catalyst here illustrated for a hydrogen molecule adsorbed in a Metal-Organic Framework, above a Zn site.

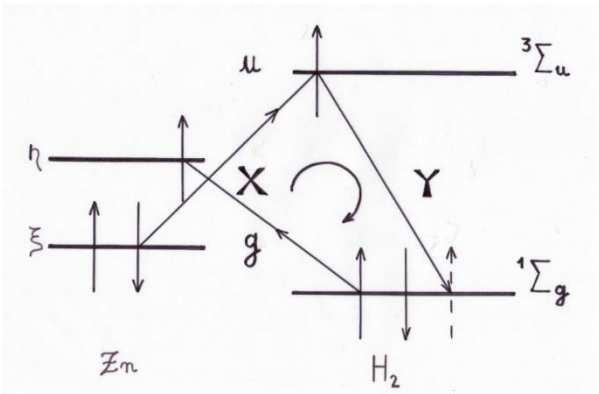

Figure 10. The XY Exchange-Coulomb conversion channel. (**a**) The molecule–solid electron exchange C = **X** excites simultaneously the molecule and the solid antibonding states (a two-electron excitation). In such an intermediate state of that singlet channel of mutual neutral states, the bonding (and antibonding) electrons have parallel spins. (**b**) In the next step of mutual electron and nuclear spin "flip-flop", the molecular electrons transfer their spin momenta by hyperfine contact **Y** to the nuclei, converting the molecule, as represented in the Figure 5.

The ortho-para process leads to a different molecule rotation and on the solid side, an exciton is emitted and propagates until mutual annihilation.

3.1.3 Three– Step Channels

The Electromagnetic Conversion channels that have been investigated for the hydrogen molecule in semiconductors and insulators complement the **XY** and **UY** catalytic steps by a third spin-orbit one **Λ**. These three-step channels correspond to a sufficient **SO** coupling (**Λ**) in the solid and sufficient scattering time. In such a process the solid relaxes before the molecule leaves and only a nuclear energy is exchanged with the solid. That channel has been particularly efficient on amorphous solid water at low temperature.
That family of processes, denoted Spin-Orbit-Coulomb-Contact **SOCY** or **ΛCY**, considers that the previous **CY** path leaves the system in a transient virtual state and complements it by an additional **SO** one, that brings back the electrons in their original ground state. The net transition is then purely nuclear, and conversion occurs at the low frequencies of several meV. The excited electron states are transients of a loop and the electron system returns to its fundamental ground state.

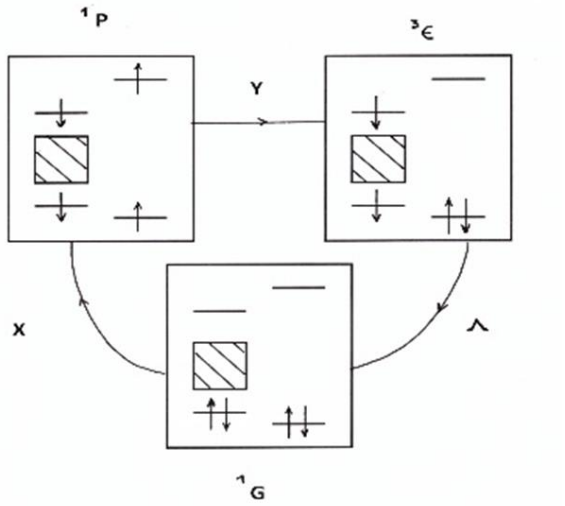

Figure 11. A Singlet Channel: the molecule-solid electron repulsion X excites simultaneously the molecule and the solid antibonding states (a two-electron excitation). In such a neutral state the bonding (and antibonding) electrons have opposite spins and the molecule rotates differently (not represented). In the next step the molecular electrons transfer their spin momenta to the nuclei by hyperfine contact Y. Finally, the spin-orbit interaction brings back the solid to its original ground state.

Inside the family **ΛCY** many channels are effective, owing to the order under which the successive perturbations apply and the nature of the virtual states visited by the electronic paths. In the path represented on the Figure 11, the mutual electron exchange step between the metal and the molecule leads to a virtual singlet. It is followed by an hyperfine contact of the excited electron with the nuclear protons that brings back the excited electron to the conduction band. Finally, the spin-orbit coupling relaxes it in the valence band.
In the Figure 12, the hyperfine contact excites the electron in a virtual triplet state and transfers the electron spin angular momentum to the nuclei, before jumping to the metal first in the conduction band and further relaxed towards the valence band by electron spin-orbit relaxation. (Another path, not herewith represented, would introduce first some magnetic excitations in the

non-magnetic solid ground state by electron spin-orbit. That **SO** coupling had already been suggested to complement electric polarization effects on the hydrogen molecule, but that molecular channel requires a complex catalytic path).

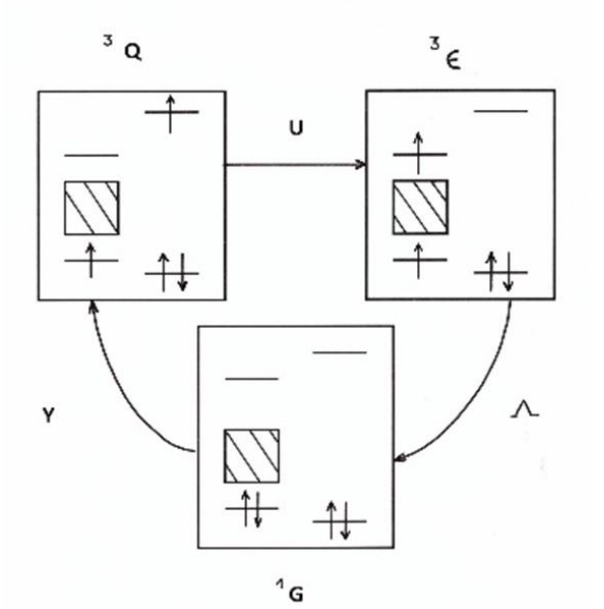

Figure 12. A Triplet Channel: An example of a solid valence electron jumping on the molecular u state by hyperfine contact (a single-electron excitation). The shifted electron and its remaining pair in the solid build a magnetic electronic state that flips the nuclear spins. The electron repulsion brings back the shifted electron to the solid through the molecule-solid bridge (the bonding of the antibonding states) emitting (or not) an exciton. Finally the spin-orbit interaction brings back the solid to its original ground state.

3.2 Symmetry breakings and selection rules

The link between the nuclear rotational and spin symmetries of molecular hydrogen depends on the electron system, in which the nuclei are embedded. In particular, the ortho- and para- varieties are different nuclear manifolds of the full electron ground state of the system complex. Conversion mixes these nuclear states through an electromagnetic interaction and thus breaks the symmetry introduced by the Pauli principle.

The o-p conversion of molecular hydrogen involves both a symmetry breaking and a thermal accommodation with the bath. As concerns the symmetry breaking, any o-p transition necessitates the change of both the rotational and spin nuclear momenta $\Delta J = \Delta I = 1$. The electron complex provides paths through transient magnetic states that break the Pauli electron and nuclear anti-symmetries and correlate the electron fluctuations to the molecule and phonon dynamics. As concerns the thermal accommodation, the non-equilibrium ortho-para ratio produces a drift on the complex that induces the successive electronic transitions. The electron system acts as a key that regulates the thermal flow between the molecule and the solid. The various conversion channels appear thus as reaction paths tunneling through transient states, branches or loops in the electronic space that must overcome different energy barriers to complete the molecule rotational and nuclear spin transitions.

Diamagnetic substrates are characterized by a catalyst ground state whose electron structure is composed of closed shells that possess neither spin nor orbital momentum. However, the non-equilibrium molecular drift can induce the conversion by a transfer of angular momentum towards catalyst magnetic excited states. Such processes include one-electron excitations from occupied orbitals to empty ones, that is from singlets to triplets. The 3 angular momenta electron spin selection rule corresponding to the one-step magnetic path then becomes (0, 1, 1) that is $\Delta S = 1$ for the catalyst, as demonstrated by Ilisca and Ghiglieno [68-71]. Two or Three main "symmetry-breaking**"** interactions have been combined to build a conversion operator.

The Coulomb repulsion denoted **C** among the solid and molecular electrons conserves the total electronic spin but might change simultaneously the electron spins of the catalyst and the molecule. **C** breaks also the molecule inversion symmetry and mixes "gerade" (g) and "ungerade" (u) states, which are respectively bonding (b) and antibonding (ab). **C** induces also the molecular rotational transition $\Delta J=1$, because the excited antibonding molecular orbital u is linked to the inter-nuclear axis and thus connects the ortho and para varieties with different rotational states.

The magnetic hyperfine contact **Y** breaks both the electron and nuclear spin angular momentum conservation: $\Delta S = \Delta I = 1$. Finally the spin-orbit **Λ** (and exchange) interactions collecting one and two electron excitations, break the solid or the molecule electron orbital and spin conservations and induce Singlet-Triplet and bonding-antibonding mixings.

In the Two-Step Reaction Paths the nuclear selection rules are satisfied successively by a first step : $\Delta J = 0$, $\Delta I = 1$ and next step $\Delta I = 0$, $\Delta J = 1$ or inversely. The reaction path of the **XY** channels, can be summarized in the molecular space by : $^1\Sigma_g(J=I=1) \rightarrow \{^3\Sigma_u(J=0, I=1) - ^3\Sigma_u(J=1, I=0)\} \rightarrow ^1\Sigma_g(J=I=0)$. That is, starting from an ortho ground state $^1\Sigma_g$ **(J = I = 1)** the path visits the excited para $^3\Sigma_u$ (S= 1, J=1, I=0) and the excited ortho $^3\Sigma_u$ (S= 1, J=1, I=0) states before ending in the final para ground state $^1\Sigma_g$ **(J = I = 0).**

Such a path mixes bonding and anti-bonding electronic states as well as singlet and triplet electron spins of the electron complex. Let us denote the orbital state (O_H, O_C)O and the spin one by (S_H, S_C)S, where the sub-indexes H is relative to the hydrogen molecule and C to the catalyst. The molecular orbital space is simplified in either the ground bonding and the excited antibonding one : O_H=(g, u), whereas the catalyst one is being reduced to one valence band V and one conduction band C : O_C= (V,C).

The exchange-contact **XY** orbital path for an insulating catalyst **:** (O_H= g, O_C=V) → (O_H= u, O_C=C) → (O_H= g, O_C=C) then combines with the spin one: (S_H= 0, S_C=0)0 → (S_H= 1, S_C=0)1 → (S_H= 0, S_C=1)1. For the metallic catalyst the orbital path remains inside the conduction band : (g, C) → (u, C) → (g, C) . Differently the charge transfer **UY** path characterized by the molecular reaction: $^1\Sigma_g(J=I=1) \rightarrow \{^2\Sigma_u(J=0, I=1) - ^2\Sigma_u(J=1, I=0)\}$

$\rightarrow {}^1\Sigma_g(J=I=0)$ is associated to an orbital path similar to the XY one but to a different spin one: (S_H= 0, S_C=0)0 $\rightarrow$ (S_H= 1/2, S_C=1/2)1 $\rightarrow$ (S_H= 0, S_C=1)1.
In both Two- Step Reaction Paths, the catalyst ends in an excited magnetic state that propagates before being disintegrated. The molecule has transferred its rotational momentum to the catalyst which become slightly magnetized. Such paths are particularly adapted to the metallic configuration where the conduction band is partly filled. Therefore, the energy exchanged by the conversion process is the o-p nuclear one of 15 meV. Differently in the case of insulator or semiconductor catalysts, the energy involved by a conversion mechanism might exceeds the eV. Therefore, these energies must be shared by the collective system. In other words, the electron energy emitted at one nanocage might be absorbed and returned by exciton scatterings or at another nanocage.
In the Three-Step Reaction Paths of the **XYΛ** channels, the molecular path is similar as previously: ${}^1\Sigma_g(J=I=1) \rightarrow \{{}^3\Sigma_u(J=0, I=1) - {}^3\Sigma_u(J=1, I=0)\} \rightarrow {}^1\Sigma_g(J=I=0)$, but the spin-orbit interaction allows the catalyst to return to its ground state. Therefore, two virtual excited states are visited as for example:

(O_H=g, O_C=V) $\rightarrow$ (O_H=u, O_C=C) $\rightarrow$ (O_H=g or u, O_C=C) $\rightarrow$ (O_H=g, O_C=V)

(S_H=0, S_C=0)0 $\rightarrow$ (S_H= 1, S_C=0)1 $\rightarrow$ (S_H= 0, S_C=1)1 $\rightarrow$ (S_H= 0, S_C=0)0

For such three-step XYΛ channels the energy exchanged by the conversion process remains the o-p nuclear one of 15 meV even for insulator catalysts of large eV gap and the electronic path remains virtual. In most cases the molecular angular momenta are exchanged with the solid except for some special scattering configurations where the returning beam might absorb part of the rotational momenta. Differently the rotational energies can be shared between the phonons and the molecular motion during the (inelastic) scattering. It is still an open question that must be examined for each experiment and hydrogen-catalyst configuration.

4 Electron and nuclear spectroscopy measurements

From the beginning of the new century, new and beautiful experiments observed and measured quite fast o-p conversion (of the order of one or a few minutes) for hydrogen physisorbed on different dielectric and diamagnetic insulators, either by "in situ" infra-red (IR) spectroscopy, or by thermal-desorption (TDS) followed by photo-ionization (REMPI), or by magnetic pulses (NMR). The materials used for hydrogen non-magnetic fast catalysis were Metal Organic Frameworks (MOF) [72-77], the dielectric amorphous solid water ASW [53,56,78,79] and polymer samples [80]. Different materials that present non-magnetic catalysis, but of much slower rate, are the semi-conductors Si and ZnO [48-51, 81-84] and fullerene samples of C_{60} [85-94]. Raman and infrared spectroscopies could observe first in 1992 the hydrogen conversion by exciting the molecular rovibronic degrees of freedom [14]. As the rotational branches were resolved, it became possible to follow the time evolution of their populations. The development of "in situ" and "site-specific" methods combine these optical measures with surface spectroscopies such as X-rays or neutron beams, thermal-or photo-induced desorption [3,4]. They became increasingly efficient in comparing molecules adsorbed on different metal, oxygen or organic surface sites [68-70] or diluted inside semi-conductors [71] and insulated cages [4].
Three nuclear methods were used to measure the concentrations of the ortho and para varieties, and their interconversion for H_2 molecules encapsulated in nanocages: (i) the IR absorption lines intensity and dynamics, (ii) Neutron scattering experiments, (iii) NMR methods are also able to measure the protons spin magnetization and their relaxation [86,89-91]. Insulator cages are able to store para-hydrogen with long dormancy (the cage shielding protects and increases the p-H_2 conservation).
The “REMPI” electronic method (Resonance Enhanced Multi Photon Ionization) measures the conversion of hydrogen combining 3 techniques: (i) initial preparation of a non-equilibrium hydrogen gas by chromatography and adsorption on a clean surface (ii) followed by a photo-stimulated desorption and (iii) a laser time-resolved analysis of the ejected molecules by a two-photon ionization of the molecular electrons [3,45-47,78,79]. The measurements on a silver surface and on solid water, at low temperature corroborated the IR observations demonstrating that non-magnetic insulating catalysts can convert non-equilibrium mixtures of hydrogen. The observed time scale of the order of 1-10 minutes is original first by its shortness. These experiments are also original by the use of optical methods to measure the o-p hydrogen conversion at the contact of a solid adsorbing structure. They sample the surface layer by irradiation, excite the vibronic degrees of freedom and are more precise than NMR.

4.1 Rotational-vibrational spectra

Some important low energy Ro-Vibrational Levels of the hydrogen molecule are represented in the Figure 13. The MOF samples were not designed for conversion purpose, but in search of micro-porous materials with high specific areas and pore volumes for hydrogen storage. The infrared lines are measured with a precision of the order of the cm^{-1} and the evolution of the ortho and para lines could be followed in real time.

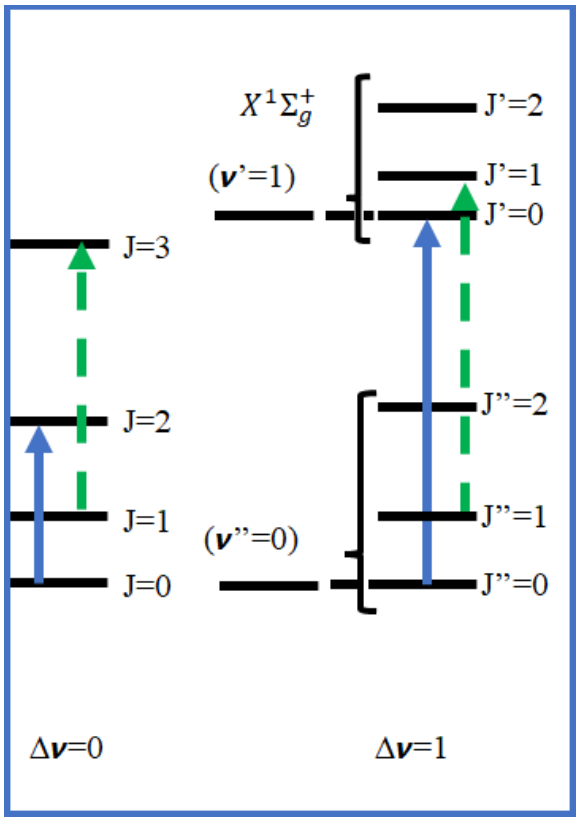

Fig. 13. Hydrogen Ro-Vibrational spectroscopy: energy levels and main rotational–vibrational lines.

4.1.1 MOF.

The measurements of o-p conversion in Metal Organic Frameworks were conducted at Oberlin College, by S. FitzGerald and coworkers, with a Diffuse Reflection Infrared Spectroscopic apparatus [72-77]. They are more precise than the ones obtained by transmission. A similar apparatus constructed in Sao Carlos is represented at the top of the Figure 14. For hydrogen physisorbed in the pores of Metal Organic Frameworks (MOF), and in particular for MOF-74 samples containing zinc metal ions, "site-specific" infra-red measures were reached by varying the amount of adsorbed hydrogen, exploring and comparing the IR lines corresponding to molecules adsorbed on different metal, oxygen or organic sites [72-77]. Hydrogen enriched in various non-equilibrium ortho concentrations being introduced, o- and p-lines are clearly identified from their dynamical behavior, as represented at the bottom of the Figure 14. The simultaneous o-decrease and p-increase of these lines follow in real time the isomers relaxation towards thermal proportions. It was also observed that conversion occurred with similar rates for molecules adsorbed on metal or oxygen sites (of the order of the minute), and that the metallic rates were enhanced by the presence of neighbor molecules adsorbed over the oxygen ions.

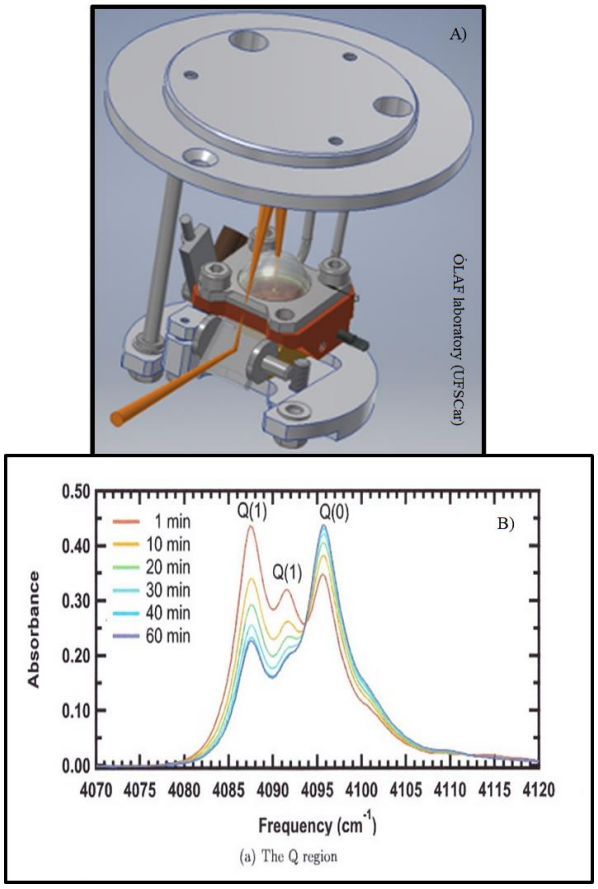

Fig. 14. Infrared spectroscopy in nanocages: A) opto-mechanical detail from the experimental setup; B) infrared intensity lines during the o-p conversion in the metal-organic framework (MOF) [72-77]. Ortho and Para Hydrogen IR Absorption Lines Time Evolution in Molecular Organic Frameworks. Ortho (red) and Para (blue) lines of Hydrogen adsorbed on MOF 74 sites (1). (The legend gives time after loading H_2 into the sample chamber). Reproduced with permission from Burkholder, B., "Catalysis of Conversion Between the Spin Isomers of H_2 by MOF-74", Oberlin College, 2009.

4.1.2 Semi-conductors.

The Infrared Spectroscopic measurements of hydrogen encapsulated in Nano-Cages were also performed for various semi-conductors to sample the formation of hydrogen molecules inside the diamagnetic structure. After annealing, the hydrogen atoms diffuse towards tetrahedral sites where they combine. As soon as the hydrogen molecules form, their nuclear spin populations come into sight and it is possible to follow their slow relaxation towards thermal concentrations over a few hours [48-51].

Hydrogen is a common and important impurity in semiconductors, which can be trapped at various sites of the host lattice. Main investigations were conducted in Dresden for silicon samples. In Si [81–84], GaAs and Ge the introduction of hydrogen in high concentrations results in the formation of extended planar defects, called platelets. It is possible to obtain interstitial H_2 in silicon compounds by cooling the Si from a melt in a hydrogen plasma. Main features of interstitial molecules in silicon are the followings: conversion times of tens to

hundreds of hours and not minutes as in noble metals or ionic insulators. The conversion of is exceptionally slow at 77 K, (about 230 h) but as the silicon structures become more disordered in K-complexes and platelets, with gaps reduced by impurities or two-dimensionality, the conversion becomes faster (by a factor ~25 for platelets). The measured rates at 300 K remain quasi-insensitive to the gap width but about 30 times faster than the one at 77 K.
Ilisca and Ghiglieno suggested an interpretation of these measurements by remarking that the two-step processes are more efficient at high temperature whereas the three-step ones, described in sections 2.3 and 3.1, are becoming increasingly faster as the temperature is lowered [71].

4.1.3 Fullerenes and Polymers.

The « Columbia » research group of Pr. Turro developed a new and fruitful molecular surgery (i) by opening the buckyballs (ii) inserting the hydrogen at high temperature and pressure through the created holes (iii) closing the holes and regenerating C_{60} at room temperature. The advancement of "molecular surgery" has succeeded for instance to trap the hydrogen molecules inside fullerene cages, and then encapsulate them in a NaY zeolite structure where each pore (diameter around 8 Å) is able to accommodate one $H_2@C_{60}$ [85,88]. Due to the large, spherical shape of the molecules, solid C_{60} has large interstitial voids making it a good host for matrix isolation. These voids come in two varieties. The sites are small enough that each will contain only one hydrogen molecule. Using infrared spectroscopy to study H_2 intercalated within a C_{60} lattice gives insight into the nature of the C_{60}–H_2 interaction. H_2 is not infra-reactive under normal conditions and so the H_2 absorption peaks in the spectra are purely due to interaction with the C_{60} host.
The conversion of hydrogen in a PCP polymer [80] was measured and studied by many complementary technics: sample preparation by chemical synthesis, structural analysis by neutron and X-ray diffraction synchrotron radiation and magnetic susceptibilities measured by a SQUID magnetometer. Hydrogen in the sample was measured by a combination of adsorption isotherm, and the Raman in situ spectroscopy was carried out by a spectrometer in the temperature range of 20–77 K. The data were registered with high counting statistics, at 35 and 65 K in the H_2 adsorbed and desorbed states, accurate charge densities and electrostatic potentials in the pores were determined by combining the maximum entropy method (MEM) and Rietveld refinement.

4.2 Nuclear magnetic resonance

The nuclear magnetic spectrum of the ortho manifold is represented on the Figure 15 together with the two neighbor para energies. The para manifold is not magnetic and thus not observed by NMR but might be deduced from the ortho one.

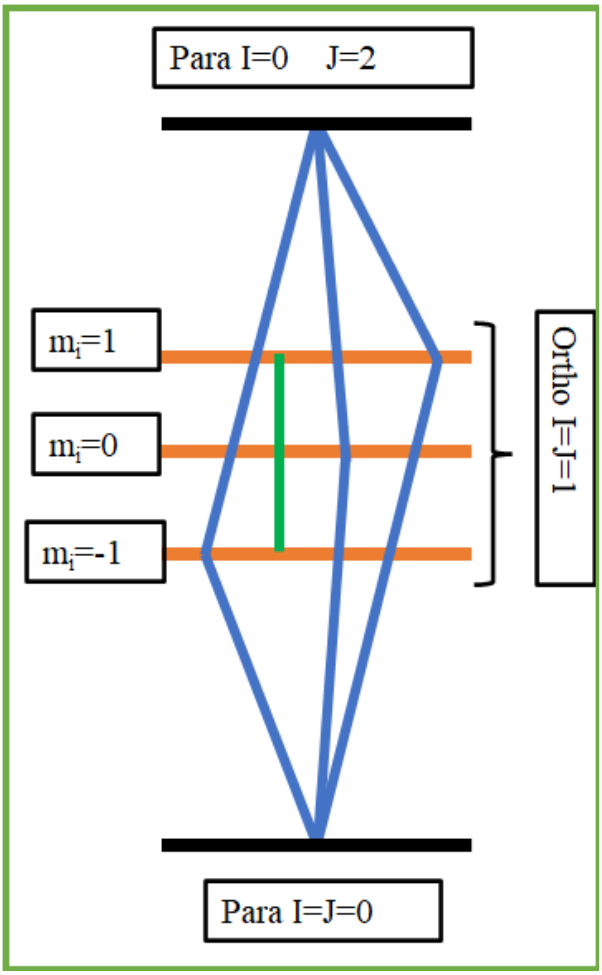

Fig. 15. Hydrogen conversion and nuclear resonance spectroscopy. The ortho manifold is amplified in comparison with the two neighbor para energies. The resonance lines in green are compared to the ortho-para line sin blue.

4.2.1 Fullerenes.

The « Columbia » research group sampled the H_2 molecules encapsulated in C_{60} cages: $H_2@C_{60}$ and measured their conversion and relaxation rates by NMR techniques [85-94]. From the temperature-dependent relaxation times analysis, it was found that H_2 reorients itself about an order of magnitude faster in solution than as a guest in $H_2@C_{60}$, as might be expected for a very small molecule tumbling in the "soft" solvent cage, compared with the closed confines of the "hard" walls of C_{60}. Thus, the incarcerated H_2 "feels" the walls of the C_{60} cage to a greater extent than in a solvent. The picture has emerged of the hydrogen molecule as a rotating gyroscope whose direction of rotation is changed by collisions with the wall faster than changes of the rotation rate.
Different methods for enriching $H_2@C_{60}$ in the para isomer have been developed: (i) Cooling a sample of the fullerene in liquid O_2 and rapidly boiling off the O_2 after low-temperature equilibrium is achieved. (ii) Attaching a functional group to the fullerene cage that can be converted to a paramagnet. Following low-temperature equilibration, the catalytic group must be rapidly back converted to the non-magnetic form. This method has been termed « a magnetic switch ». (iii) Low-

Temperature photoexcitation of a fullerene containing trapped H_2 to paramagnetic triplets. Rapid decay of the triplet and re-excitation of the endofullerene lead to equilibration of the sample at low temperature. This method has been termed « a photochemical on–off switch » for o-p conversion [91].

4.2.2 Viscous Organic Solutions

The conversion processes induced by solids might be compared with those occurring inside liquids [12,13]. and particularly in viscous solutions, since it gives information on how the hydrogen molecule behaves and "thermalize" when enclosed in a surrounding cage [4]. The first important NMR measurements of H_2 conversion catalyzed by paramagnetic ions in deuterated solvents were performed in 2005. Matsumoto and Espenson measured the o-p rate constants by means of the proton NMR in deuterated solvents at 298 K [61]. NMR spectroscopy has proven to be one of the most powerful methods for understanding the mechanisms of hydrogenation reactions; indeed, it is widely used in catalysis for the characterization of homogeneous and heterogeneous catalysts, reactants and products in different phases, reaction intermediates.

The subject of "singlet and triplet relaxations" and their inter-relations must also be replaced in a wider context: conversion and relaxation rates were measured in fullerene cages and organic solvents by NMR. Recent experiments have measured the conversion rate of hydrogen molecules dissolved in paramagnetic organic solvents. The proton signals display negative peaks during an initial period. The interpretation given by Ilisca describes a polarization effect: the transient behavior of the nuclear spins directed on the average along the magnetic electronic spins as represented on the Figure 16 [67]. It relies on a non-equilibrium ortho drift and gives access to the transient nuclear magnetization, function of the sample magnetic concentration. The hydrogen molecules and the magnetic impurities recurrently stick together for a short time.

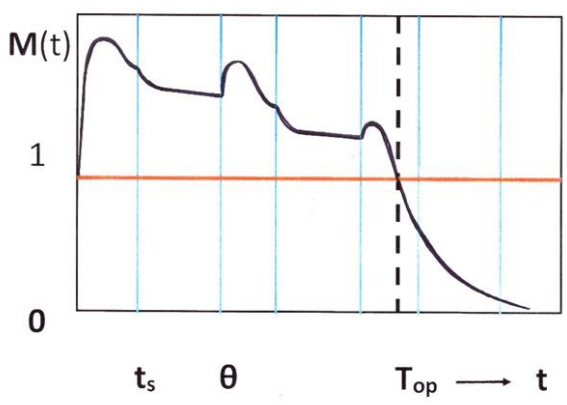

Fig. 16. The relative nuclear magnetization of molecular hydrogen diluted in a magnetic viscous organic solution departs from its equilibrium value (M=0) reached for times much longer than the conversion time T_{op}. t_s represents a sticking time and θ the interval between two scatterings.

The hydrogen molecule is then confined inside a nanocage whose size depends both on the solvent viscosity and the attraction of the metallic magnetic impurity.

Consequently, the relative values of the relaxation times are related to the ratio of the long- and short-range interactions, as well as to the size of the nanocage and the time spent by the molecule within the cage. Important ratios are deduced: conversion versus relaxation characteristic times and collision versus sticking time intervals. The contact interaction is found stronger than the long range and fluctuating dipolar one for magnetically concentrated samples during the short sticking of the colliding partners, but weaker for diluted ones.

4.3 Electron Spectroscopies

In 2003 a Japanese team introduced a "REMPI" method (Resonance Enhanced Multi Photon Ionization), briefly summarized on the Figure 16, to measure the conversion of hydrogen on a silver surface [45]. Shortly later, o-p conversion of hydrogen adsorbed on amorphous ice (ASW) was observed by different means [56]. A remarkable preparation of ortho-hydrogen by chromatography was followed by thermal stimulated desorption and a laser beam time-resolved analysis (REMPI). Time evolution of the hydrogen isomers is registered, and their relaxation is observed to occur in about 6 minutes. These figures related to the water oxygen ions compare favorably with the MOF-oxygen rates, although slower. Moreover, preliminary conversion observed on MOF, occurred also on these ASW samples.

REMPI methods corroborated the efficiency of oxygen ions and attributed the fast o-p conversion observed on amorphous ice to their giant surface electric fields [56]. In particular low symmetry systems like amorphous, disordered, porous materials… display numerous localized states, "dangling" or "open" bonds, in the insulating gaps. Some of them might be occupied but a number of them are empty and might be excited by the molecular scattering.

It is known for long that the electric field E is very intense at the surface of the ASW samples, of the order of a few V/ Å, and very inhomogeneous (steep gradients of 1-10 V. $Å^{-2}$). They polarize the hydrogen molecules and affect their rotational behavior. From the initial and noticeable hydrogen preparation, such a field effect was used by passing the hydrogen flow through a chromatographic column to separate the o- and p-isomers and prepare a non-equilibrium gas. Thereafter adsorption on the ice sample, and desorption by thermal pulses the gas is analyzed by a laser beam. The rotational state-selectivity of the REMPI method is highly sensitive. The observed conversion, occurring in between 6 and 20 minutes, is due to the oxygen and hydroxyl ions of the surface water molecules. It allows the unique opportunity to compare the efficiencies of different oxygen ions.

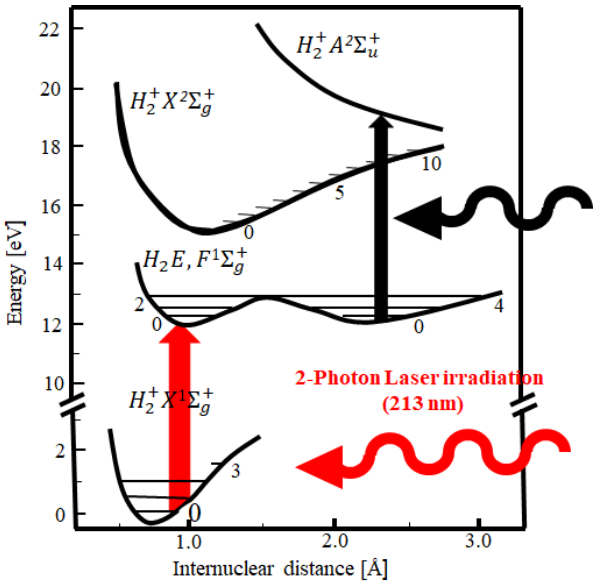

Fig. 17. Resonance Enhanced Multi-Photon Ionization (REMPI). A first Pump Laser 2-photon irradiates the ejected molecules and a second laser by ionizing them differentiates the ortho and para varieties.

Interpretation of H_2 Conversion on Ag (111) at 7 K, by Ilisca in 1990, relied on the two-step **XY** and **UY** mechanisms as described in the sections 2.2 and 3.1 [39-44]. The interpretation of H_2 Conversion on Amorphous Solid Water ASW, and its temperature dependence around 15 K, published in 2012 relied on the three-step **ΛXY** and **ΛUY** mechanisms described in the sections 2.3 and 3.1 [95]. Both rely on the mixings of electronic excited Spin-Orbitals. Does that pattern (o-p rates of a few minutes) characterize a new class of o-p diamagnetic catalysts? Can their different surface dielectric properties be sampled by hydrogen conversion?

The conversion rates over the oxygen ASW sites have been compared to the ones above with the triangle of oxygen ions characteristic of the MOF secondary site which were found faster than the ASW ones by a factor of about 10. Ilisca and Ghiglieno attributed that MOF pattern to the number of σ and π oxygen covalent bonds interacting with a hydrogen molecule adsorbed above the middle of the triangle [69].

5 Concluding comments

The physical catalysis of hydrogen presents the striking effect of reducing dramatically the interconversion time, longer than the age of the universe for isolated molecules, to a few seconds, minutes or hours when an hydrogen sample (gaseous or liquid) is brought into contact with a solid catalyst. In the present conference report we attributed such catalytic efficiency to the symmetry breaking introduced by the solid to pass round the peculiar selection rules of the molecular hydrogen assigned by the Pauli Principle.

Up to the end of the last century, hydrogen conversion on solids was observed exclusively on magnetic catalysts able to create magnetic fields, inhomogeneous on atomic scale, able to diphase the nuclear spin precession of the 2 protons. Moreover, no experimental tool was available to observe directly the conversion on surfaces and the measured rates on a macroscopic scale were some mixing between the molecular sticking, the adsorption-desorption cycle and the magnetic rates.

The present century gave rise to new and efficient non-magnetic catalysts, new experimental methods leading to precise measurements and to new theoretical interpretations and concepts. Moreover, the rush toward a clean and renewable energy has driven hydrogen towards new applied researches and developments. The present conference reports such a renewal and the following concluding comments summarizes its main features.

Let us start by the new radiative methods (Raman, Infra-Red or REMPI) that are now sufficiently precise to distinguish the ortho and para lines, disentangle the rotational properties from the vibronic ones and measure their relaxation patterns. It is now possible to follow in real time the hydrogen adsorption, their filling on different sites and conversion rates (which allows for example to distinguish between metallic and oxygen sites). New neutron imaging registers the diffusion and conversion of hydrogen inside the porous structure of catalysts and cover them with a camera. New nuclear magnetic pulses are also able to polarize the proton spins and follow their relaxation, whereas STM observations are becoming precise enough to follow the rotational patterns of hydrogen on metallic surfaces.

Simultaneously these new experimental means appeared able to observe the hydrogen isomers time evolution on new non-magnetic catalysts and report conversion on diamagnetic surfaces on the time scales of one-ten minutes. Such observations produced a shock since it turned upside down the previous theory, established in 1933, of the absolute necessity of a magnetic catalyst to break the Pauli Principle. First observed on noble metals around 1980 then on semi-metals, then after 2000 on semiconductors and lastly on insulators, polymers, fullerenes, organic compounds… the conversion patterns were different from the magnetic ones. They raised questions about the influence of the surface ionicity and electric field; more generally on the electronic distribution all over the surrounding cage. Multiple information on the catalytic rates implied the disentanglement of what pertained to the solid and the molecular structure. On the solid side, the importance of disordered structures (aggregates, super molecules, amorphous or powders) raised questions on a possible correlation of the conversion mechanism with the catalyst disorder. Ones pertain to the category of nanocages developed by molecular surgery methods for which the concept of multiple valence bond introduced by Van der Walle should be considered. Distinctly, 2d and 3d crystal structures offer properties for which collective effects are part of the catalytic mechanism. On the side of molecular chemistry, non-equilibrium phenomena and irreversible shifts such as negative temperature effects and transient nuclear spin polarizations in organic solutions were observed thanks to these new electromagnetic measurements.

In parallel, new concepts and electromagnetic conversion channels have been provided to explore and interpret these experimental renewals. What

differentiates the described channels is the path followed by the quantum system to introduce an electron spin inside the molecule. Once inside, the electron spin becomes particularly efficient in exerting a differential torque on the proton spins. In strongly adsorbing surfaces, as in porous confining structures or inside nanocages, the solid and molecular electron clouds overlap, and the hydrogen nuclei feel a complex electronic structure. It is usual to apply perturbation methods to the physisorption of hydrogen molecules rotating almost freely, in particular for the very weak electron-nuclear hyperfine interactions. Such methods lead to a series expansion of successive electron interactions that have been translated in terms of successive contributions of virtual intermediate and excited electronic states. Each one has been identified as a catalytic channel characterized by successive symmetry breakings. If such a series expansion converges rapidly remains an open question.

As experiences are becoming more precise and new substrates more adsorbing, the o-p conversion which was a prototype of physical catalysis is moving towards the field of electro-chemical reactions. This necessitates new concepts in terms of fractional charges, electronegativity and electron correlations in complex scatterings. It must be noticed that little is known about the correlation between electronic fluctuations and the ortho and para chemical potentials difference.

More generally the conversion phenomena obey physical principles similar to those developed in the chemically induced nuclear and electron polarization (CIDNP and CIDEP), or to luminescent and phosphorescent effects such as the disintegration of a singlet into two excited triplets or inversely in the triplet-triplet annihilations occurring in radical pairs.

The very long lifetimes of the hydrogen nuclear spin isomers has applications in various contexts for research or industrial purposes, detailed in Ilisca's review [4]. For practical applications, the preparation of hydrogen molecules in a pure para state and their polarization transfer lead to giant NMR (Nuclear Magnetic Resonance) signals used in medical imaging (PASADENA effect). In Astrophysics, the ortho-para concentration helps to date the formation of interstellar clouds, and in chemistry it is used to follow the transient states of chemical reactions. For industrial applications, nuclear conversion appears as an interesting tool to develop nano-porous materials with high selectivity. The main challenge concerns the practical use of the H_2 internal energy, which requires condensed storage forms. The liquefaction process also uses conversion stages which represent from 18% to 53% of the total liquefaction work owing to the number of stages.

In conclusion, the theoretical framework herewith summarized, registers and classifies the new information gained by the last ten years of experiments. A number of conversion channels, herewith described, lead to a reasonable approach of new phenomena of hydrogen conversion on diamagnetic and insulating surfaces composed of closed shells of oxygen and metal ions.

References

1. A. Farkas, *Orthohydrogen, Parahydrogen and Heavy Hydrogen*; Cambridge University Press: Cambridge, UK (1935)
2. E. Ilisca, *Ortho-Para Conversion of Hydrogen on Surfaces*. Prog. Surf. Sci. **41**, 213–336 (1992)
3. K. Fukutani, T. Sugimoto, *Ortho-Para Conversion of Molecular Hydrogen in Physisorption States on Solid Surfaces*. Prog. Surf. Sci. **88**, 279 (2013)
4. E. Ilisca, *Hydrogen Conversion in Nanocages*. Hydrogen **2**, 160–206 (2021)
5. E.P. Wigner, *Über die paramagnetische Umwandlung von Para-Orthowasserstoff. III*. Part I Phys. Chem. Part II Solid State Phys. **23**, 126–130 (1997)
6. G. E. Schmauch, A. H. Singleton, *Technical Aspects of Ortho-Parahydrogen Conversion*. Ind. Eng. Chem. **56**, 20–31 (1964)
7. E. Ilisca, E., S. Sugano, *A new channel in ortho-para H_2 conversion*. Phys. Rev. Lett. **57**, 2790 (1986)
8. E. Ilisca, *Magneto-optic and magneto-catalytic effect*. J. Magn. Soc. Jpn. **11**, 13 (1987)
9. E. Ilisca, S. Sugano, *Optical studies in ortho-para conversion of a hydrogen molecule on a magnetic surface*. Chem. Phys. Lett. **149**, 20–23 (1988)
10. B. I. Lundquist, *Electron Transfer at Surfaces*. In Electronic Processes at Solid Surfaces, E. Ilisca, K. Makoshi, Eds.; (World Scientific Pub Co Pte Ltd: Singapore city, Singapore, 1996)
11. M. Bloom, *Nuclear spin relaxation in hydrogen*. Physics **23**, 378–388 (1957)
12. S. E. Nielsen, J. S. Dahler, *Paramagnetic Catalysis of the Ortho-Parahydrogen Conversion*. J. Chem. Phys. **46**, 732 (1967)
13. P. W. Atkins, M. J. Clugston, *Ortho-Para Hydrogen conversion in Paramagnetic Solutions*. Mol. Phys. 27, 1619 (1974)
14. H. G. Hixson, M. J. Wojcik, M.J., M. S. Devlin, J. P. Devlin, V. Buch, *Experimental and Stimulated Vibrational Spectra of H_2 adsorbed in Amorphous Ice*. J. Chem. Phys. **97**, 753–767 (1992)
15. A. Züttel, A. Borgschulte, L. Schlapbach, *Hydrogen as a Future Energy Carrier*. (WILEY-VCH Verlag, GmbH & Co: Hoboken, NJ, USA, 2008)
16. D. H. Weitzel, *Standards*. J. Res. Nat. Bur. **A60**, 2840 (1958)
17. *Survey study of the efficiency and economics of hydrogen liquefaction*. Linde-Union Carbide (Report: Seadrift, TX, USA, 1975)
18. E. Ilisca, E. *Theoretical calculation of a new effect in ortho-para H_2 conversion on magnetic surfaces*. Phys. Rev. Lett. **24**, 797 (1970)
19. E. Ilisca, *Experimental evidence for a new effect in ortho-para H_2 conversion on magnetic surfaces*. Phys. Lett. **33A**, 247 (1970)
20. E. Ilisca, *A Simple Example of Ferromagnetic Catalysis*. J. Vac. Sci. Technol. **25**, 183 (1971)
21. E. Ilisca, A. P. Legrand, *Theoretical rates and correlation functions in o-p hydrogen conversion on paramagnetic surfaces*. Phys. Rev. B **5**, 4994 (1972)
22. E. Ilisca, E. Gallais, *Orientation effect of the surface magnetization of ferromagnetic catalysts on the ortho-para H_2 conversion*. Phys. Rev. B **6**, 2858 (1972)

23. Y. Ishii, S. Sugano, *Ortho-para conversion of hydrogen on magnetic surfaces*. Surf. Sci. **127**, 21–34 (1983)
24. M. Fujiwara, K. Niki, T. Okano, K. Fukutani, *Ortho-Para H_2 Conversion on Cr_2O_3 (0001)/Cr (110) surfaces*. J. Physics, Conf. Ser. **200**, 22038 (2010)
25. P. Avouris, D. Schmeisser, J.E. Demuth, *Observation of Rotational Excitations of hydrogen adsorbed on Ag surfaces*. Phys. Rev. Lett. **48**, 199 (1982)
26. S. Andersson, J. Harris, J. *Observation of Rotational Transitions for H_2, D_2 and HD Adsorbed on Cu(100)*. Phys. Rev. Lett. **48**, 545 (1982)
27. R. E. Palmer, R. F. Willis, *Rotational States of Physisorbed Hydrogen on Graphite*. Surf. Sci. **179**, L1 (1987)
28. K. G. Petzinger, D.J. Scalapino, *Para- to Ortho-Hydrogen Conversion on Magnetic Surfaces*. Phys. Rev. B **8**, 266–279 (1973)
29. E. Ilisca, *Introduction to a theory of paramagnetic catalysis: the magnetic field effect*. Phys. Rev. Lett. **40**, 1535 (1978)
30. E. Ilisca, M. Debauche, J. L. Motchane, *Quantum formulation of a magneto-catalytic reaction*. Phys. Rev. B **22**, 687–701 (1980)
31. E. Ilisca, M. Debauche, *Surface spin polarization by rotational libration*. Surf. Sci. **144**, L449 (1984)
32. E. Ilisca, *Theory of ortho-parahydrogen conversion catalyzed by "d" electrons*. Chem. Phys. Lett. **168**, 289 (1990)
33. K. Makoshi, E. M. R. Ilisca, *Dipolar and contact processes in H_2 o-p conversion on ionic surfaces*. J. Phys. Condens. Matter **5**, 7325 (1993)
34. M. Rami, K. Makoshi, E. Ilisca, *Physical Conversion of H_2 adsorbed on Cr_2O_3/Al_2O_3*. Appl. Surf. Sci. **68**, 197 (1993)
35. E. Ilisca, S. Paris, S. *A charge transfer process in o-p H2 conversion induced by 3d impurities on a perovskite*. Surf. Sci. **363**, 347–353 (1996)
36. E. Ilisca, K. Bahloul, *Orbital Paramagnetism and o-p H_2 Conversion*. J. Phys. B At. Mol. Opt. Phys. **29**, 607 (1996)
37. S. Paris, E. Ilisca, *Electron-Nucleus Resonances and Magnetic Field Acceleration in H_2 conversion*. J. Phys. Chem. **A103**, 4964 (1999)
38. E. Ilisca, S. Paris, *Magnetic Field Acceleration of the o-p H_2 conversion on Transition Oxides*. Phys. Rev. Lett. **82**, 1788 (1999)
39. E. Ilisca, *Ortho-para H_2 conversion on a cold Ag(111) metal surface*. Phys. Rev. Lett. **66**, 667–670 (1991)
40. E. Ilisca, *Ortho-para hydrogen conversion on noble metals*. Mod. Phys. Lett. B **5**, 1191–1198 (1991)
41. E. Ilisca, *Molecule-surface complexes and catalytic reaction*. Surface Science **242**, 470 (1991)
42. E. Ilisca, *H_2 conversion on noble metals*. J. Phys. I **1**, 1785 (1991)
43. E. Ilisca, *Orbital process in o-p H_2 conversion on noble metals*. J. Phys. Cond. Matter **4**, 297 (1992)
44. E. Ilisca, *Towards an hyperfine measure of noble metals Image "Surface states"*. Optics Comm. **89**, 399 (1992)
45. K. Fukutani, K. Yoshida, M. Wilde, W. A. Diño, M. Matsumoto, T. Okano, *Photostimulated Desorption and Ortho-Para Conversion of H_2 on Ag Surfaces*. Phys. Rev. Lett. **90**, 096103 (2003)
46. M. Sakurai, T. Okano, Y. Tuzi, *Ortho-para conversion of n-H_2 physisorbed on Ag(111) near two-dimensional condensation conditions*. Appl. Surf. Sci. **33–34**, 245–251 (1998)
47. K. Niki, T. Kawauchi, M. Matsumoto, K. Fukutani, T. Okano, *Mechanism of Ortho-Para H_2 Conversion on Ag surfaces*. Phys. Rev. B **77**, 201404 (2008)
48. E. V. Lavrov, J. Weber, *Ortho and Para Interstitial H_2 in Silicon*. Phys. Rev. Lett. **89**, 215501 (2002)
49. A. W. R. Leitch, V. Alex, J. Weber, *Raman Spectroscopy of Hydrogen Molecules in Crystalline Silicon*, Phys. Rev. Lett. **81**, 421 (1998)
50. E. R. Pritchard, M. J. Ashwin, J. Tucker, R. C. Newman, *Isolated interstitial hydrogen molecules in hydrogenated crystalline silicon*, Phys. Rev. B **57**, R15048 (1998)
51. E. E. Chen, M. Stavola, W. B. Fowler, P. Walters, *Key to Understanding Interstitial H_2 in Si*, Phys. Rev. Lett. **88**, 105507 (2002)
52. P. L. Chapovsky, E. Ilisca, E. *Theory of nuclear-spin conversion in ethylene*. Phys. Rev. A **63**, 62504 (2001)
53. H. Ueta, N. Watanabe, T. Hama, A. Kouchi, *Surface Temperature Dependence of Hydrogen Ortho-Para Conversion on Amorphous Solid Water*. Phys. Rev. Lett. **116**, 253201 (2016)
54. M. Tsuge, T. Hama, Y. Kimura, A. Kouchi, N. Watanabe, *Interactions of Atomic and Molecular Hydrogen with a Diamond-like Carbon Surface: H_2 Formation and Desorption*. Astrophys. J. **878**, 23 (2019)
55. N. Watanabe, M. Tsuge, *Experimental Approach to Physicochemical Hydrogen Processes on Cosmic Ice Dust*. J. Phys. Soc. Jpn. **89**, 051015 (2020)
56. T. Sugimoto, K. Fukutani, *Electric-field-induced nuclear-spin flips mediated by enhanced spin–orbit coupling*. Nat. Phys. **7**, 307 (2011)
57. S. K. Estreicher, K. Wells,P.A. Fedders, P. J. Ordejon, *Dynamics of interstitial hydrogen molecules in crystalline silicon*. J. Phys. Condens. Matter **13**, 6271–6283 (2001)
58. C. M. Cunningham, H. L. Johnston, H.L. The surface catalysis of the ortho-to para-conversion in liquid hydrogen by paramagnetic oxides on alumina. J. Am. Chem. Soc. **80**, 2377 (1958)
59. T. Das, S.-C. Kweon, I. W. Nah, S. W. Karng, J.-G. Choi, I.-H. Oh, *Spin conversion of hydrogen using supported iron catalysts at cryogenic temperature*. *Cryogenics* **69**, 36–43 (2015)
60. J. H. Kim, S. W. Karng, I-H. Oh, I. W. Nah, *Ortho-para hydrogen conversion characteristics of amorphous and mesoporous Cr_2O_3 powders at a temperature of 77 K*. Int. J. Hydrog. Energy **40**, 14147–14153, (2015)
61. M. Matsumoto, J. H. Espenson, *Kinetics of the Interconversion of Parahydrogen and Orthohydrogen Catalyzed by Paramagnetic Complex Ions*. J. Am. Chem. Soc. **127**, 11447–11453 (2005)
62. E. Sartori, M. Ruzzi, MN. J. Turro, J. D. Decatur, D. C. Doetschman, R. G. Lawler, A. L. Buchachenko, Y. Murata, K. Komatsu, *Nuclear Relaxation of H_2 and $H_2@C_{60}$ in Organic Solvents*. J. Am. Chem. Soc. **128**, 14752–14753 (2006)
63. C. Aroulanda, L. Starovoytova, D. Canet, *Longitudinal Nuclear Spin Relaxation of Ortho- and Para-Hydrogen*

Dissolved in Organic Solvents. J. Phys. Chem. A **111**, 10615–10624 (2007)
64. D. Canet, S. Bouguet-Bonnet, C. Aroulanda, F. Reineri, *About Long-Lived Nuclear Spin States Involved in Para-Hydrogenated Molecules*. *J*. *Am*. *Chem*. *Soc*. **129**, 1445–1449 (2007)
65. E. Sartori, M. Ruzzi, R. G. Lawler, R.G.; N. J. Turro, *Nitroxide Paramagnet-Induced Para−Ortho Conversion and Nuclear Spin Relaxation of H_2 in Organic Solvents*. J. Am. Chem. Soc. **130**, 12752–12756 (2008)
66. C. Terenzi, S. Bouguet-Bonnet, d. Canet, *Direct 1H NMR evidence of spin-rotation coupling as a source of para-ortho-H_2 conversion in diamagnetic solvents*. *J*. *Chem*. *Phys*. **146**, 154203 (2017)
67. E. Ilisca, *Nuclear Spin Relaxation, Conversion, and Polarization of Molecular Hydrogen in Paramagnetic Solvents*. J. Phys. Chem. C **123**, 16631–16640 (2019)
68. E. Ilisca, *Hydrogen conversion on non-magnetic insulating surfaces*. EPL Europhys. Lett. **104**, 18001 (2013)
69. E. Ilisca, F. Ghiglieno, *Electron exchanges in nuclear spin conversion of hydrogen physisorbed on diamagnetic insulators*. Eur. Phys. J. B **87**, 235–264 (2014)
70. E. Ilisca, F. Ghiglieno, *Nuclear conversion theory: molecular hydrogen in non-magnetic insulators*. *R*. *Soc*. *Open Sci*. **3**, 160042 (2016)
71. E. Ilisca, F. Ghiglieno, *Electronuclear paths in the nuclear conversion of molecular hydrogen in silicon*. Chem. Phys. Lett. **667**, 233–237 (2017)
72. S. A. FitzGerald, T. Yildirim, L. J. Santodonato, D. A. Neumann, J. R. D. Copley, J. J. Rush, F. Trouw, *Quantum dynamics of interstitial H_2 in solid C_{60}.* Phys. Rev. B **60**, 6439–6451 (1999)
73. S. A. FitzGerald, S. Forth, M. Rinkoski, *Induced infrared absorption of molecular hydrogen in solid C60*. Phys. Rev. B **65**, 140302 (2002)
74. S. A. Fitzgerald, H. O. H. Churchill, P.M. Korngut, C. B. Simmons, Y. E. Strangas, *Cryogenic apparatus for diffuse reflection infrared spectroscopy with high-pressure capabilities*. Rev. Sci. Instrum. **77**, 93110 (2006)
75. S. A. FitzGerald, K. Allen, P. Landerman, J. Hopkins, J. Matters, R. Myers, J. L. C. Rowsell, *Quantum dynamics of adsorbed in the microporous framework MOF-5 analyzed using diffuse reflectance infrared spectroscopy*. Phys. Rev. B **77**, 224301 (2008)
76. S. A. FitzGerald, J. Hopkins, B. Burkholder, M. Friedman, J. L. C. Rowsell, *Quantum dynamics of adsorbed normal- and para-H_2, HD, and D2 in the microporous framework MOF-74 analyzed using infrared spectroscopy*. Phys. Rev. B **81**, 104305 (2010)
77. S. A. FitzGerald, B. Burkholder, M. Friedman, J. B. Hopkins, C. J. Pierce, J. M. Schloss, B. Thompson, J. L. C. Rowsell, *Metal-Specific Interactions of H_2 Adsorbed within Isostructural Metal Organic Frameworks*. J. Am. Chem. Soc. **133**, 20310 (2011)
78. M. Chehrouri, J.-H. Fillion, H. Chaabouni, H. Mokrane, E. Congiu, F. Dulieu, E. Matar, X. Michaut, J. L. Lemaire, *Nuclear Spin Conversion of Molecular Hydrogen on Amorphous Solid Water in the Presence of O_2 traces*. Chem. Phys. **13**, 2172 (2011)
79. K. Kuwahata, T. Hama, A. Kouchi, N. Watanabe, *Signatures of Quantum-Tunneling Diffusion of Hydrogen Atoms on Water Ice at 10 K*. Phys. Rev. Lett. **115**, 133201 (2015)
80. T. Kosone, A. Hori, E. Nishibori, Y. Kubota, A. Mishima, M. Ohba, H. Tanaka, K. Kato, J. Kim, J. A. Real, et al., *Coordination nano-space as stage of hydrogen ortho-para conversion*. R. Soc. Open Sci. **2**, 150006 (2015)
81. M. Hiller, E. V. Lavrov, J. Weber, *Raman scattering study of H_2 in Si*. J. Phys. Rev. B **74**, 235214 (2006)
82. M. Hiller, E. V. Lavrov, J. Weber. *Ortho-Para Conversion of Interstitial in Si*. Phys. Rev. Lett. **98**, 055504 (2007)
83. C. Peng, M. Stavola, W. B. Fowler, M. Lockwood, *Ortho-para transition of interstitial H_2 and D_2 in Si*. Phys. Rev. B **80**, 125207 (2009)
84. S. Koch, E. V. Lavrov, J. Weber, T*owards understanding the hydrogen molecule in ZnO*. J. Phys. Rev. B **90**, 205212 (2014)
85. Y. Murata, M. Murata, K. Komatsu, *100% Encapsulation of a Hydrogen Molecule into an Open-Cage Fullerene Derivative and Gas-Phase Generation of H_2@C60*. J. Am. Chem. Soc. **125**, 7152–7153, (2003)
86. M. Carravetta, Y. Murata, M. Murata, I. Heinmaa, R. Stern, A. Tontcheva, A. Samoson, Y. Rubin, K. Komatsu, M. H. Levitt. *Solid-State NMR Spectroscopy of Molecular Hydrogen Trapped Inside an Open-Cage Fullerene*. J. Am. Chem. Soc. **126**, 4092–4093, (2004)
87. K. Komatsu, M. Murata, Y. Murata. *Encapsulation of Molecular Hydrogen in Fullerene C_{60} by Organic Synthesis*. Science **307**, 238–240 (2005)
88. M. Murata, Y. Murata, K. Komatsu. *Synthesis and Properties of Endohedral C_{60} Encapsulating Molecular Hydrogen*. J. Am. Chem. Soc. **128**, 8024–8033 (2006)
89. M. Carravetta, O. G. Johannessen, M. Levitt, I. Heinmaa, R. Stern, A. Samoson, A. Horsewill, Y. Murata, K. Komatsu, *Cryogenic NMR spectroscopy of endohedral hydrogen-fullerene complexes*. J. Chem. Phys. **124**, 104507 (2006)
90. M. Carravetta, A. Danquigny, S. Mamone, F. Cuda, O. G. Johannessen, I. Heinmaa, K. Panesar, R. Stern, M. C. Grossel, A. J. Horsewill et al. *Solid-state NMR of endohedral hydrogen–fullerene complexes*. Chem. Phys. **9**, 4879–4894 (2007)
91. N. J. Turro, J. Y.-C. Chen, E. Sartori, M. Ruzzi, A. Marti, R. Lawler, S. Jockusch, J. López-Gejo, K. Komatsu, Y. Murata, *The Spin Chemistry and Magnetic Resonance of H_2@C60. From the Pauli Principle to Trapping a Long Lived Nuclear Excited Spin State inside a Buckyball*. *Accounts Chem*. *Res*. **43**, 335–345 (2010)
92. M. Ge, U. Nagel, D. Hüvonen, T. Rõõm, S. Mamone, M. Levitt, M. Carravetta, Y. Murata, K. Komatsu, J.Y.-C. Chen et al., *Interaction potential and infrared absorption of endohedral H_2 in C60*. J. Chem. Phys. **134**, 054507 (2011)
93. J.Y.-C. Chen, Y. Li, M. Frunzi, X. Lei, Y. Murata, R. G. Lawler, N. J. Turro, *Nuclear Spin Isomers of guest molecules in H_2@C_{60} and other fullerenes*. Phil. Trans. R. Soc. A **371**, 20110628 (2013)
94. S. Mamone, M. R. Johnson, J. Ollivier, S. Rols, M. H. Levitt, A. J. Horsewill, *Symmetry-breaking in the*

H_2@C_{60} endofullerene revealed by inelastic neutron scattering at low temperature. Chem. Phys. **18**, 1998–2005 (2015)
95. E. Ilisca, *Electromagnetic nuclear spin conversion: Hydrogen on amorphous solid water*. Chem. Phys. Lett. **713**, 289–292 (2018)
96. C. R. Bowers, D. P. Weitekamp, *Transformation of symmetrization order to nuclear-spin magnetization by chemical reaction and nuclear magnetic resonance*. *Phys*. *Rev*. *Lett*. **57**, 2645–2648 (1986)
97. F. D. Natterer, F. Patthey, H. Brune, *Distinction of Nuclear Spin States with the Scanning Tunneling Microscope*. Phys. Rev. Lett. **111**, 175303 (2013)